# Density-functional and Monte Carlo study of O/Mo(110): Structures and desorption

N. V. Petrova and I. N. Yakovkin*
*Institute of Physics of National Academy of Sciences of Ukraine, Prospect Nauki 46, Kiev 03028, Ukraine*
(Received 13 June 2007; revised manuscript received 20 July 2007; published 1 November 2007)

Structures of oxygen layers on the Mo(110) surface and desorption kinetics have been investigated by means of density-functional theory and generalized gradient approximation calculations and Monte Carlo simulations. It has been found that triply coordinated hollow sites are favorable for oxygen adatoms. All energies of lateral interactions, used in the Monte Carlo simulations of the formation of oxygen structures, are found to be positive, which means that neither trio interactions nor explicit attraction between oxygen adatoms is needed to explain the formation of the $p(2\times1)$ oxygen structure. Simulated scanning tunneling microscopy (STM) images reveal a strong dependence of the relative brightness of images of O adatoms on the sample bias voltage. In particular, protrusions in STM images of oxygen-covered Mo(110) surface, obtained with a negative sample bias, cannot be attributed to images of substrate Mo atoms, but correspond to increased electron density induced by the overlap of atomic densities of neighboring oxygen adatoms. The estimated binding energy between adsorbed O atoms and Mo surface substantially exceeds the binding energy between two oxygen atoms in a free molecule. This feature is suggested to be responsible for the atomic form of oxygen desorption from the Mo(110) surface.

DOI: 10.1103/PhysRevB.76.205401 PACS number(s): 68.43.Bc, 68.43.Fg, 68.43.Vx, 68.35.Bs

## I. INTRODUCTION

Adsorption and desorption of oxygen on transition metal surfaces play an important role in many surface phenomena such as corrosion and various chemical reactions. Detailed understanding of the interaction of oxygen with transition metal surfaces is therefore essential for further progress in the development of layered and nanostructure materials with desirable properties.

The (110) surfaces of bcc transition metals have been the most suitable for experimental studies of oxygen adsorption,[1–15] in a large part due to close-packed structures of these surfaces which provide their high stability with regard to possible adsorption-induced reconstruction.[5–17] In particular, an oxygen-covered Mo(110) surface does not show any noticeable reconstruction even on heating to relatively high temperatures (above 1000 K), whereas a Mo(112) surface, under the same conditions, reconstructs by forming complex surface structures.[18,19] It is worth noting that the formation of an oxide layer on the Mo(110) surface, very recently studied by low energy electron diffraction (LEED), scanning tunneling microscopy (STM), and density-functional theory (DFT),[20] can be accomplished by heating to 1000 °C in $O_2$ atmosphere at $1\times10^{-6}$ Torr, but not by heating the sample with an adsorbed oxygen layer. The $MoO_2$ formation implies diffusion of oxygen atoms into the surface, which can be accomplished only for high oxygen coverages, perhaps, because of the low probability of diffusion and related surface reconstruction.

The interpretation of LEED patterns is not always straightforward, in particular, when the coverage cannot be determined unambiguously. Thus, actual structures of adsorbed oxygen layers on W(110) were a subject of debates[5–7] until recent STM studies[8] confirmed the formation of the linear chains of oxygen adatoms, oriented along the diagonals of the W(110) rectangular-centered unit cell, pertinent to forming the $p(2\times1)$ structure. On the Mo(110) surface, at $\theta=0.5$, oxygen also forms the $p(2\times1)$ structure.[15] However, the $p(2\times2)$O structure on the Mo(110) surface forms at $\theta=0.25$,[10] while for O/W(110), the $p(2\times2)$ LEED pattern is believed to originate from the "empty-sites" structure[7] at $\theta=0.75$.

The $p(2\times2)$O structure on Mo(110) was not revealed in STM images,[15] while at intermediate coverages, STM images show the formation of a complex structure and, at $\theta=0.5$, of the $p(2\times1)$ structure. It should be noted that the interpretation of STM images of oxygen-covered surfaces is complicated by the strong dependence of the STM current on the distribution of electronic density, which for systems with strong interactions, as in the case of oxygen adsorption on transition metal surfaces, can be rather complex.

Because of the difference in electronic structures (in particular, occupations of the *d* shells), oxygen adsorption and desorption occur significantly different for different transition metals. While dissociation of an oxygen molecule on the Pt(111) surface requires some activation energy,[21–23] on the Mo(110) and W(110) surfaces, oxygen molecules readily dissociate, resulting in chemisorption of oxygen atoms even at very low (4 K) temperatures.[3] The difference between electronic structures of Pt(111) and Mo(110) [or W(110)] reveals itself also in the different forms of oxygen desorption. From the Pt(111) surface, oxygen desorbs in a molecular form,[22,23] while for the Mo(110) [as well as W(110)], experiments indicate predominantly an atomic form of oxygen desorption.[1,2] Corresponding temperature-programed desorption (TPD) peaks appear at ~700 K for the associative desorption of oxygen from Pt(111),[22,23] while about 2000 K for atomic desorption from Mo(100) and W(110) surfaces.[1,2]

Associative desorption requires a reunion of two atoms, which seems quite improbable both right on the surface and far from the surface. Indeed, should two atoms on the surface occur sufficiently close to each other to form the molecular bond, they would immediately dissociate back because of the influence of the substrate electrons. On the other hand, far

 

from the surface, evaporated atoms hardly would find each other to form a molecule. Thus, first-principles calculations for hydrogen on the Mo(110) surface[24] have revealed that the association of the hydrogen atoms can be accomplished only in a narrow range of distances from the surface, about 0.5 Å. Properties of chemisorbed oxygen on transition metal surfaces, obviously, significantly differ from those of hydrogen adlayers, in particular, because of a strong lateral interaction between O adatoms. The lateral interaction can be considered as a superposition of a screened Coulomb or dipole-dipole and indirect interactions[25–28] and results, for example, in forming a $(2\times2)$O structure at saturating 0.25 coverage on Pt(111).[28]

In the present study, we a suggest a consistent picture of the formation of the O adlayer structures and oxygen desorption from the Mo(110) surface using the methods (DFT repeat-slab calculations and Monte Carlo simulations) and models successfully applied previously to the H/Mo(110),[24] (CO+O)/Pt(111),[28,29] and O/Pt(111)[30] systems.

## II. METHOD OF CALCULATIONS

The repeat-slab DFT semirelativistic calculations were carried out with the ABINIT code,[31] using Troullier-Martins norm-conserving pseudopotentials[32] and generalized gradient approximation for exchange-correlation energy in Perdew-Burke-Ernzerhof form.[33] The quality of the potentials was further verified by the estimation of the lattice constant for the bulk Mo bcc crystal as well as of the bond length and binding energy of an oxygen molecule.

Oxygen is known as a "difficult case" in pseudopotential calculations because of a slow convergence of the total energy with regard to the number of plane waves included in the basis set. Thus, while the 1 millihartree (0.027 eV) convergence for bulk Mo was readily achieved with an energy cutoff of 20 hartree (40 Ry), giving the minimum in the total energy for the lattice constant of 3.16 Å (in good agreement with the experimental value of 3.15 Å), to obtain well-converged values of total energy for an oxygen molecule and for the O/Mo(110) adsorption system, the cutoff was increased to 36 hartree. It is worth noting that the convergence of 0.01 Å for the estimated bond length in the oxygen molecule, 1.23 Å, consistent with the experimental value of 1.21 Å, was achieved already with a 20 hartree cutoff.

Another problem with the correct evaluation of the energy of an oxygen atom as well as with the related binding energy in the $O_2$ molecule appears because of the triplet ground state of the O atom. This feature requires spin-polarized calculations "in a big box," which implies either a ferromagnetic or an antiferromagnetic state of the model O crystal (to avoid these problems, Kiejna and Nieminen[34] suggested the esteem of the O atom energy as one-half of the energy of the $O_2$ molecule). While the energy of the $O_2$ molecule is the same in the spin-polarized and paramagnetic calculations, the binding energy in the $O_2$ molecule without taking account of the spin polarization is dramatically overestimated. In contrast, calculations for a model antiferromagnetic O crystal, built from separate O atoms in the triplet states, provide a reasonable esteem of the binding energy, 5.33 eV, consistent with experiment.

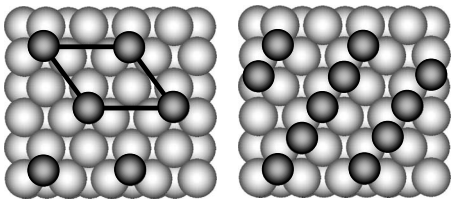

FIG. 1. The $p(2\times2)$ and $p(2\times1)$ oxygen structures, forming at $\theta=0.25$ and $\theta=0.5$ on the Mo(110) surface. All O adatoms occupy equivalent triply coordinated hollow sites.

Obviously, by increasing the number of atoms in the unit cell, the computational time significantly increases, so that it is desirable to adopt as thin a slab as possible while keeping the most important structure and electronic properties unchanged with respect to those of the surface of a bulk (semi-infinite) crystal. The three-, four-, five-, and seven-layer slabs were tested for convergence of the surface properties. Optimization of the atomic positions for a clean Mo(110) surface indicates contraction (about 5%, in good agreement with *I-V* LEED results[35] and similar calculations[16,17]) of the topmost Mo(110) surface layer with respect to related interplane distance in bulk Mo (2.244 Å, adopted accordingly to calculated 3.16 Å optimal lattice constant of the bulk Mo). There are only minor relaxation shifts found for the second and third layers, which seems to be a result of the close-packed structure of the Mo(110) surface. Even three Mo(110) layers (provided that the lowest one is kept fixed) well reproduce the relaxation and also the local density of states at the surface. Hence, while the evaluation of binding energies was performed for a five-layer Mo(110) substrate, potentials of lateral interactions for various distances between oxygen adatoms and related possible paths of the association of oxygen atoms into a molecule were estimated for a rigid three-layer substrate slab with the $(2\times2)$ rhombic surface unit cell [shown in Fig. 1(a)].

The O atoms were adsorbed on various sites on one side of the slab. The positions of the oxygen atoms and Mo atoms of two surface layers were optimized until the forces on atoms converged to less than 0.02 eV/Å. No explicit compensation for the resulting dipole moments, sometimes used to improve the convergence in the calculations for strongly polar surfaces to account for the asymmetry of the potential at the two sides of the film, was exploited in the present study. In fact, the efficient screening of local fields in the O/Mo(110) adsorption system makes such corrections insignificant provided that the spacing between the slabs is taken to be sufficient to eliminate interaction between the surfaces through the vacuum gap. In the present calculations, the convergence of the total energy was verified also with respect to the width of the vacuum gap between the slabs and was concluded to be satisfactory for the vacuum gap about the thickness of the slab.

The ABINIT code[31] provides a tool for generating efficient *k*-point lattices, which in simple cases can be reduced to the familiar Monkhorst-Pack[36] sets of special points in the Brillouin zone (BZ). The efficiency of the BZ sampling is con-

trolled by a "real-space length" parameter related to the inverse spacing between the $k$ points in the mesh. The convergence with respect of the BZ sampling, using various $k$-point lattices, was carefully verified, and the $4\times4\times1$ Monkhorst-Pack set of $k$ points was found sufficient, providing in all cases the required 0.002 hartree convergence of total energies as well as about 0.02 Å accuracy of atomic positions.

For the modeling of the formation of oxygen structures and the desorption from the Mo(110) surface, we used our set of Monte Carlo programs, verified in simulations for various adsorption systems.[28–30,37–39] Briefly, the method, which explores the standard Metropolis algorithm for the lattice gas model,[40] takes into account the long-range dipole-dipole and indirect interactions between particles adsorbed on the 36 $\times60$ lattice with periodic boundary conditions. Rearrangement of the particles ("surface diffusion") was performed by movements ("jumps") of randomly chosen adatoms to neighboring sites.

The probability of a jump, $\exp(-\Delta E/kT)$, depends on the difference of energies $\Delta E$ of lateral interaction with other adsorbed particles for the initial and final configurations. When the jump leads to a gain in energy ($\Delta E<0$) or an estimated probability exceeds a random number, the jump is accomplished. Otherwise, the attempt of the jump fails and the particle remains at the original site. After a sufficient number of accomplished jumps (usually, about 30 per particle), the system achieves thermodynamical equilibrium. Depending on the temperature, the adsorbed particles can form ordered structures or, at higher temperatures, the film is disordered.

Relative intensities of LEED reflections are estimated within the kinematical approximation:

$$I(h,k)=\left|\sum_{n}\exp\{2\pi i(hx_n+ky_n)\}\right|^2. \quad (1)$$

The summation is performed over occupied sites with $x_n$ and $y_n$ coordinates, defined in terms of fractions of the simulated fragment of the surface. $h$ and $k$ denote reciprocal space coordinates. Calculations performed for a lattice of $h$ and $k$ points resemble the distribution of reflections over the screen, and the simulated LEED pattern is depicted by circles whose sizes indicate the intensity.[37–39]

Modeling of the TPD spectra was conducted using a routine algorithm (see, e.g., Ref. 37 and references therein) with a stepwise 10° increase of temperature. The rate of desorption was determined as the number of the $O_2$ molecules or O atoms evaporated at a given temperature per second. The probability of evaporation of a particle was defined as $W=\nu\exp(-E_{des}/kT)$, with desorption activation energy $E_{des}$ and preexponent factor $\nu$.

## III. RESULTS

### A. Structures of O layers on Mo(110)

Optimization of atomic positions of adsorbed oxygen atoms and Mo atoms of the two surface layers leads, on average, to a "backward" relaxation of the Mo(110) surface; that is, after the optimization, the spacing between the surface and next to surface Mo(110) layers resembles (within 0.5%) that for the (110) planes in a bulk Mo crystal. A rather strong interaction between adsorbed oxygen atoms and Mo surface atoms results in a minor ($\sim1\%$) surface corrugation, which, nonetheless, decreases the total energy of the system and therefore gives rise to the estimated binding energies. The length of the O-Mo bond is found to be in the range of 1.08–1.12 Å with related O-Mo interlayer distance of about 1.3 Å, consistent with values suggested in Ref. 12.

Calculations of total energies have shown that triply coordinated (quasi-three-fold) hollow sites of the Mo(110) surface are strongly favorable for oxygen atoms both for the $p(2\times1)$ and $p(2\times2)$ structures (Fig. 1). It should be noted that while the quasi-three-fold position of oxygen atoms in the $p(2\times1)$ structure is consistent with high-resolution electron-energy-loss spectroscopy (HREELS) results[11,13,14] and is in line with $I$-$V$ LEED results and calculations for O/W(110),[5] it was suggested[13] that, at $\theta=0.25$, oxygen adatoms on the Mo(110) should prefer bridge sites. Present calculations, however, show that even in the $p(2\times2)$ structure, positions of oxygen adatoms in the triply coordinated sites are favored for 0.2 eV per atom with regard to long-bridge sites. Such a significant difference of total energies cannot be attributed to possible errors and inclines one to accept the interpretation of HREELS with some precaution. In particular, because of the strong lateral interactions, the frequencies of vibration of adsorbed O atoms might be different for different coverages, which does not necessarily indicate that oxygen adatoms would occupy different adsorption sites. It is worth noting that in a recent study of $MoO_2$ layers on the Mo(110) surface,[20] the threefold sites were found favorable also for oxygen atoms at the interface.

Simulations of STM images, using the Tersoff-Hamann method,[41] provide insight into the origin of protrusions and dark holes observed in the images of the O/Mo(110) adsorption system. Usually, with a positive sample bias $V_s$, oxygen adatoms are imaged as dark holes (see, e.g., Refs. 8, 9, and 15). This feature can be attributed to a relatively low, with respect to the surface Mo atoms, local density of states (LDOS) on the oxygen adatoms in the energy range from $E_F$ to $E_F+V_s$ (Fig. 2).

On the other hand, with a negative $V_s$, the STM images of the O/Mo(110) will strongly depend on the bias. With a small negative bias voltage, oxygen adatoms still should be imaged dark because of a low LDOS on the oxygen atoms near $E_F$. With −2 V sample bias, some electrons, localized on oxygen adatoms (though, probably, originated from the bonding with the Mo substrate), will give rise to STM current and, therefore, the images of O adatoms may become bright. With a −6 V bias, the STM current will be controlled predominantly by the high oxygen-induced LDOS peak at −6 eV [see Fig. 2(a)], and the oxygen adatoms will be imaged as protrusions. These arguments are illustrated in Figs. 3(a) and 3(b) by simulated STM images of the $p(2\times2)$O structure on Mo(110) surface and calculated distributions of electronic densities in the normal plane for two characteristic bias voltages, −6 and −1 V.

It should be noted that protrusions in STM images of oxygen-covered Mo(110), obtained either with positive or

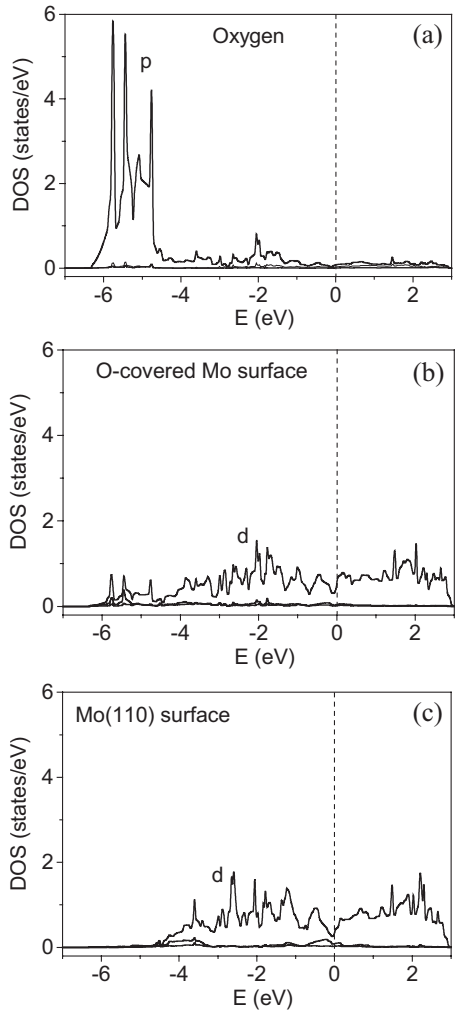


FIG. 2. LDOS: (a) on the oxygen adatom, (b) on Mo atom of the topmost layer of oxygen-covered Mo(110) surface, and (c) for a clean Mo(110) surface.

negative (−1 V) sample bias [when O atoms are imaged dark, Fig. 3(b)], cannot be attributed to images of substrate Mo atoms [Fig. 3(c)]. Rather, these protrusions correspond to increased electronic density, induced by the overlap of atomic densities of neighboring oxygen adatoms, enhanced due to the interaction with the substrate Mo(110) surface.

Usually, the conditions of STM experiments are adapted for the particular structure to obtain the best available resolution and contrast, which are controlled by the bias and tunneling current. In the Tersoff-Hamann method,[41] the related resistance of the barrier is simulated by adjustment of the tip distance from the surface (which does not necessarily correspond to the actual tip-surface distance in real STM experiments). Thus, by increasing the tip-surface distance, both resolution and contrast of the images, obtained with the fixed −1 V sample bias, decrease, while the vicinity of oxygen adatoms is still imaged dark. With decreasing distance (that mimics the increase of the tunneling current), electrons, localized on O adatoms, come to play, and therefore, oxygen adatoms in STM images will appear as protrusions.

A fragment of the STM image of a clean Mo(110) surface, obtained by Okada *et al.*,[15] is shown in the inset of Fig. 3(c),

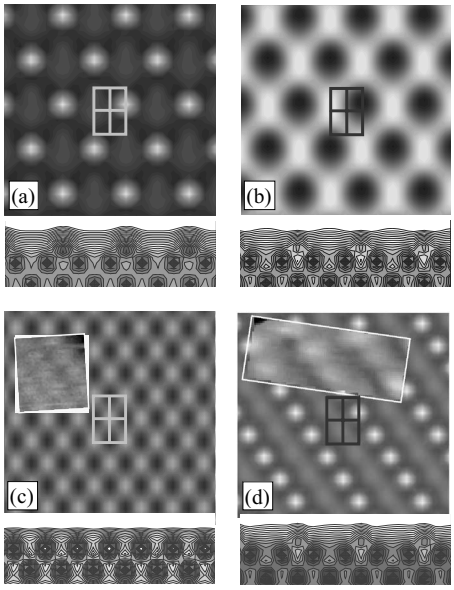


FIG. 3. Model STM images of oxygen structures on the Mo(110) surface. With bias voltage (a) $V_s=-6$ V, oxygen atoms are imaged as bright protrusions, while with (b) $V_s=-1$ V as dark holes. The STM images (c) of a clean Mo(110) surface and (d) of the $p(2\times1)$O structure, simulated with $V_s=-1$ V bias voltage, contain insets showing fragments of the real STM images (adapted from Ref. 15). Corresponding distributions of electronic densities in the normal plane are shown below the panels. The centered rectangles on the images denote the unit cell of the Mo(110) surface.

which presents a model picture simulated with the −1 V sample bias that was used in the experiment. In the model STM image of the $p(2\times1)$O structure on Mo(110) surface [Fig. 3(d)], simulated with the same bias and tip-surface distance as for the clean Mo(110), oxygen atoms are imaged as protrusions. This feature might seem rather unusual, but indicates that the fragment of STM image of the Mo(110) surface [shown in the inset of Fig. 3(d)], which corresponds, presumably, to remaining oxygen,[15] can be explained as forming the $p(2\times1)$O structure.

### B. Lateral interaction and low energy electron diffraction patterns for O layers on Mo(110)

Formation of the $p(2\times2)$O and $p(2\times1)$O structures on Mo(110) originates from a delicate balance of lateral interactions between oxygen adatoms. Relative energies of the lateral interactions that are critical for the formation of the $p(2\times1)$O structure at $\theta=0.5$ have been evaluated with DFT calculations of total energies for various positions of O adatoms. It has been found that the $p(2\times1)$ structure is favored for ~0.2 eV per atom with regard to the honeycomb structure as well as to more uniform asymmetric structures.

Energies of lateral interactions for various distances between oxygen adatoms, adopted in Monte Carlo simulations of the formation of the $p(2\times2)$O and $p(2\times1)$O structures, are denoted by symbols in Fig. 4. The chosen set of parameters can be well approximated by a screened Coulomb potential with account of Friedel oscillations,[28] which might be

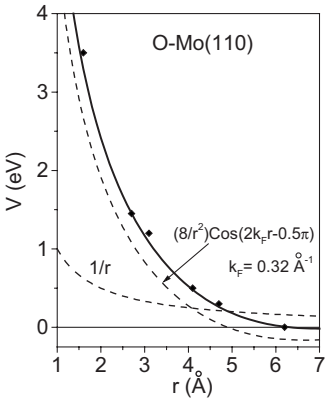


FIG. 4. Potential of the lateral interaction vs the distance between oxygen adatoms on the Mo(110) surface. The energies of the pairwise interactions, used in the Monte Carlo simulations, are denoted by symbols. The chosen set of parameters can be approximated by the sum of potentials of Coulomb and indirect interactions.

indicative of the origin of the lateral interaction between oxygen adatoms on the Mo(110) surface.

It should be emphasized that all the energy parameters used in the simulations are positive, that is, correspond to repulsion between O adatoms. Nonetheless, not only the formation of the $p(2\times2)$O structure at $\theta=0.25$ [Figs. 5(a) and 5(b)], but also the formation of a single-domain $p(2\times1)$O structure at $\theta=0.5$ [Fig. 5(c)] is readily reproduced. We underscore here that no trio interactions or some artificial anisotropy was invoked to explain the formation of these structures, as was suggested in the pioneering Monte Carlo studies of forming a $p(2\times1)$O structure on W(110).[42] The single-domain $p(2\times1)$ structure, shown in Fig. 5(c), corresponds to the formation of linear chains of oxygen atoms, oriented along one of the diagonals of the rectangular-centered Mo(110) unit cell, and therefore, only related beams appear in the corresponding LEED pattern [Fig. 5(d)]. In practice, the $p(2\times1)$ structure of the adsorbed O layer will contain domains of two equivalent orientations of the chains along the diagonals of the Mo(110) unit cell. This situation can be reproduced in Monte Carlo simulations performed either with slightly decreased parameter of lateral interaction along the diagonals or at lower temperatures. In both cases, certain "freezing" of oxygen chains [which prevents the formation of a single-domain structure around a randomly appeared "core," that is, at borders of a small island of the $p(2\times1)$ structure] results in the formation of smaller domains of the $p(2\times1)$ structure [Fig. 5(e)]. Simulated LEED pattern for this structure contains reflections, corresponding to double period along the diagonals in real space, but not along the [110] direction [Fig. 5(f)]. This feature is consistent also with LEED results for the $p(2\times1)$O structure on W(110),[5] and can be used to distinguish between the formation of the $p(2\times2)$ and multidomain $p(2\times1)$ structures [cf. Fig. 5(b)].

With somewhat increased parameter of the lateral interaction along the chains, another structure is formed [Fig. 5(g)]. This honeycomb structure still corresponds to $\theta=0.5$, but the

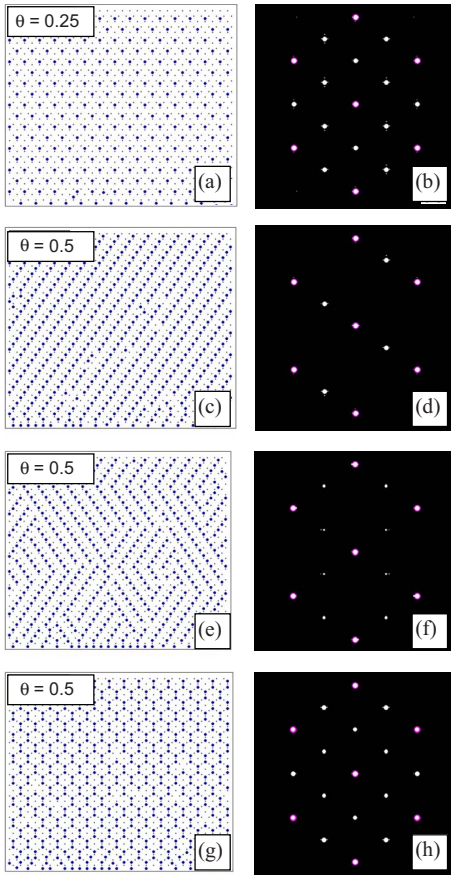


FIG. 5. (Color online) Formation of oxygen structures on the Mo(110) surface. Snapshots obtained in the course of Monte Carlo simulations are depicted in the left panels, while related model LEED patterns are shown at the right. [(a) and (b)] Formation of the $p(2\times2)$O structure. [(c) and (d)] Formation of a single domain of the $p(2\times1)$O structure with linear chains of oxygen atoms, oriented along the diagonal of the rectangular-centered Mo(110) unit cell. Note that corresponding beams appear only along one of the diagonals. [(e) and (f)] Formation of several equivalent domains of the $p(2\times1)$ structure. The LEED pattern, calculated for this structure, contains reflections, corresponding to a double period along the diagonals in real space, but not along the [−110] direction. [(g) and (h)] The forming honeycomb structure at $\theta=0.5$. The holes in the comb form the $p(2\times2)$ structure, which is reproduced in the LEED pattern.

"holes" in the combs form the $p(2\times2)$ structure and the corresponding LEED patterns show the $p(2\times2)$ structure [Fig. 5(h)], which, at first glance, might correspond to $\theta=0.75$ coverage (because of presumed 0.25 "coverage" of empty sites). In fact, however, the number of triply coordinated sites is twice the number of Mo atoms of the Mo(110) surface, so that the formation of the $p(2\times2)$ structure at $\theta=0.75$ seems problematic.

### C. Oxygen desorption from Mo(110)

The binding energy $E_b$ (positive) can be defined as the difference of total energies of the system in initial and final states, i.e., of Mo(110) with adsorbed oxygen ($E_{\mathrm{Mo+O}}$) and of

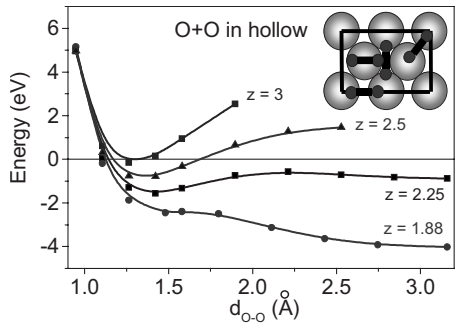


FIG. 6. Dependencies of potential energies on distances between oxygen atoms $d_{O\text{-}O}$ for several typical distances $z$ from the surface ($z=0$ corresponds to the plane passing though centers of the surface atoms). The energy of the system with a free oxygen molecule sufficiently far from the surface defines the zero of the energy scale. The inset shows possible symmetric orientations of the precursor $O_2$ molecules with respect to the surface unit cell: long-bridge $x$, long-bridge $y$, short-bridge $x$, and top $x$.

the separated substrate ($E_{Mo}$) and desorbed oxygen atom ($E_O$):

$$-E_b = E_{Mo+O} - E_O - E_{Mo}. \quad (2)$$

Optimization of the surface and next to surface atomic layers resembles surface relaxation, which is important for the estimation of the changing energy of the substrate with and without oxygen. To obtain thus defined binding energy, calculations of the total energies have been performed both for clean surfaces and for the surfaces covered with $p(2\times2)$O layers. The binding energy for an oxygen atom in a triply coordinated site is found to be 6.99 eV.

The surface relaxation and binding energies are found to be largely independent of the thickness of the substrate slab. In particular, the electronic structure of the Mo(110) surface, due to quite effective screening, can be well reproduced already with a "rigid" (that is, with fixed positions of Mo atoms) three-layer slab, which was used for purposes of searching for possible paths of the association of oxygen atoms in the $(2\times2)$ rhombic surface unit cell [shown in Fig. 1(a)].

Possible symmetric orientations of the precursor $O_2$ molecules with regard to the Mo(110) surface can be described as long-bridge $x$, long-bridge $y$, short-bridge $x$, and top $x$. These four configurations have been investigated with respect to the dependence of potential energy on the distance between oxygen atoms $d_{O\text{-}O}$, estimated for several typical distances $z$ from the surface (Fig. 6).

For distances about 2.0 Å from the surface, the potential becomes rather flat; that is, repulsive lateral interaction between oxygen adatoms vanishes. Hence, two O atoms can approach each other, forming a precursor $O_2$ molecule which can either dissociate back or desorb from the surface. The behavior of the oxygen molecule near the Mo(110) surface is illustrated in Fig. 7 by contour maps of calculated distributions of electronic density in the normal plane crossing the oxygen atoms. Shown distributions were obtained for two characteristic distances from the surface, $z=2.25$ Å and $z=1.75$ Å, with fixed $d_{O\text{-}O}=1.34$ Å distance between the oxygen atoms. Both configurations do not resemble an equilibrium state. For $z=2.25$ Å, the repulsion between oxygen atoms is small (0.0325 hartree/bohr) and increases as the molecule approaches the surface (0.0846 hartree/bohr for $z=1.75$ Å). Nonetheless, for both distances from the surface, there is a significant attraction of the oxygen atoms to the Mo(110) surface (0.024 68 hartree/bohr for $z=2.25$ Å and 0.0084 hartree/bohr for $z=1.75$ Å), and therefore, the molecule will spontaneously dissociate with subsequent chemisorption of the oxygen atoms.

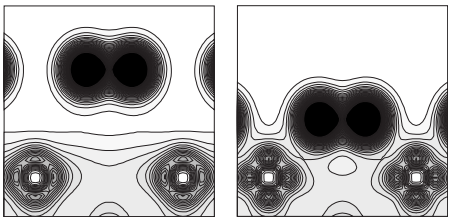

FIG. 7. Distributions of electronic densities for the precursor oxygen molecule near the Mo(110) surface. The distributions have been obtained for two characteristic distances from the surface, (a) $z=2.25$ Å and (b) $z=1.75$ Å, with fixed $d_{O\text{-}O}=1.34$ Å distance between the oxygen atoms.

Activation energy $E_{des}$ of an associative desorption can be estimated from the sum of energies required for the desorption of two oxygen atoms from the triply coordinated sites of the surface minus the gain in energy, $q$, due to the formation of the molecule:

$$E_{des} = 2E_b - q = 2(6.99) - 5.33 = 8.65 \text{ eV}. \quad (3)$$

Hence, an associative desorption of oxygen from the Mo(110) surface can be ruled out, because the required energy $E_{des}$ substantially exceeds the binding energy $E_b$ of oxygen atoms with the surface, and therefore, oxygen will desorb as separate atoms. Such a situation will occur in all cases when the binding energy with a surface exceeds the binding energy between oxygen atoms in a free molecule. For example, the binding energy for O on W(112) is about 7 eV,[43] so that only atomic phase desorption is possible. In contrast, for O on Pt(111), the binding energy is 3.7 eV,[30] and therefore, oxygen desorbs in a molecular form (associative desorption).

Both possible channels of oxygen desorption, that is, atomic and associative, were accounted for in Monte Carlo simulations of TPD spectra. Simulated TPD spectrum (Fig. 8) is characterized by a single peak at ~2000 K, which corresponds to the atomic form of desorption. With the preexponent factor $\nu=10^{13}$ s$^{-1}$ (which can be attributed to typical frequencies of vibrations of adsorbed atoms), the proper position of the peak is achieved with the desorption activation energy of about 6 eV, in agreement with the value derived (assuming the same $\nu$) from experiment.[2] DFT calculations are known for a certain overestimate of binding energies (see, e.g., Ref. 44); nonetheless, with the estimated value of the binding energy for O adatoms in the triply coordinated hollow sites on the Mo(110) surface, $E_b=6.99$ eV, the cor-

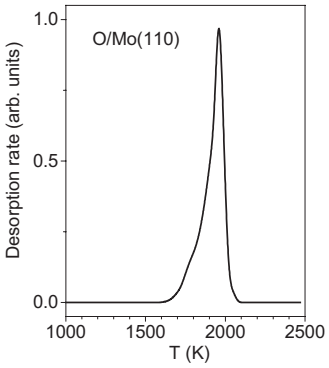


FIG. 8. Monte Carlo simulations of TPD spectra. Obtained spectrum has a single peak that corresponds to the atomic form of desorption with preexponent factor $\nu=10^{15}$ s$^{-1}$ and activation energy of 6.99 eV, obtained from the DFT calculations for the binding energy of O adatoms in the triply coordinated sites.

rect peak position can readily be obtained with the preexponent factor $\nu=10^{15}$ s$^{-1}$.

## IV. CONCLUSION

Results of calculations of total energies ultimately suggest that triply coordinated hollow sites of the Mo(110) surface are strongly favorable for oxygen atoms both for the $p(2\times1)$ and $p(2\times2)$ structures. The $p(2\times1)$O structure, forming at $\theta=0.5$, is found to be favored with regard to other possible structures (such as a honeycomb structure). These results are in agreement with recent STM study of oxygen adlayers on the Mo(110) surface as well as with LEED patterns observed for this system. All energies of lateral interactions, used in the Monte Carlo simulations of the formation of oxygen structures, are found to be positive, which means that neither trio interactions nor explicit attraction between oxygen adatoms is needed to explain the formation of the $p(2\times1)$ oxygen structure.

Simulated STM images reveal a strong dependence of relative brightness of images of O adatoms on actual conditions of experiment. In particular, with a small negative sample bias voltage, oxygen adatoms will be imaged dark, while with higher bias, they can be seen as bright protrusions. This feature results from different space distributions of states that give rise to STM current for different bias voltages. It should be emphasized that protrusions in STM images of O/Mo(110), obtained with a negative sample bias, cannot be attributed to images of substrate Mo atoms. Rather, the influence of the Mo(110) substrate reveals itself in the induced peaks in LDOS on O adatoms and the related real-space redistribution of the states.

Oxygen desorbs from the Mo(110) surface predominantly in atomic form, that is, without association of oxygen atoms into molecules. This feature is explained by a strong bonding between adsorbed O atoms and Mo surface, which substantially exceeds the binding energy in a free oxygen molecule. In general, there is a simple criterion which controls whether desorption of diatomic gases will be associative or atomic: If the binding energy with a substrate exceeds that in a free molecule, desorption will be atomic; otherwise, adatoms will associate into precursor molecule with subsequent desorption in a molecular form.

*Corresponding author; yakov@iop.kiev.ua

[1] Yu. G. Ptushinskii and B. A. Chuikov, Surf. Sci. **6**, 42 (1967); **7**, 90 (1967).
[2] N. P. Vas'ko, Yu. G. Ptushinskii, and B. A. Chuikov, Surf. Sci. **14**, 448 (1969).
[3] Yu. G. Ptushinskii, Low Temp. Phys. **30**, 1 (2004).
[4] L. H. Germer and J. W. May, Surf. Sci. **4**, 452 (1966).
[5] M. A. Van Hove and S. Y. Tong, Phys. Rev. Lett. **35**, 1092 (1975).
[6] M. G. Lagally, J. C. Buchholz, and G.-C. Vang, J. Vac. Sci. Technol. **12**, 213 (1975).
[7] T. Engel, H. Niehus, and E. Bauer, Surf. Sci. **52**, 237 (1975); E. Bauer and T. Engel, *ibid.* **71**, 695 (1978).
[8] K. E. Johnson, R. J. Wilson, and S. Chiang, Phys. Rev. Lett. **71**, 1055 (1993).
[9] R. Koller, W. Bergermayer, G. Kresse, C. Kovicka, M. Schmid, J. Redinger, R. Podloucky, and P. Varga, Surf. Sci. **512**, 16 (2002).
[10] E. Bauer and H. Poppa, Surf. Sci. **127**, 243 (1983); K. Grzelakowski, I. Lyuksyutov, and E. Bauer, *ibid.* **216**, 472 (1989).
[11] J. Kröger, S. Lehwald, and H. Ibach, Phys. Rev. B **58**, 1578 (1998).
[12] J. Kröger, T. Greber, and J. Osterwalder, Surf. Sci. **459**, 173 (2000).
[13] M. L. Colaianni, J. G. Chen, W. H. Weinberg, and J. T. Yates, Jr., Surf. Sci. **279**, 211 (1992).
[14] C. Xu and D. W. Goodman, J. Phys. Chem. **100**, 1753 (1996).
[15] A. Okada, M. Yoshimura, and K. Ueda, Surf. Sci. **601**, 1333 (2007).
[16] B. Kohler, P. Ruggerone, and M. Scheffler, Phys. Rev. B **56**, 13503 (1997).
[17] D. Proskurin, A. Nikolaychik, I. P. Koval, and I. N. Yakovkin, Phys. Status Solidi B **243**, 584 (2006).
[18] T. McAvoy, J. Zhang, C. Waldfried, D. McIlroy, P. Dowben, O. Zeybek, T. Bertrams, and S. Barrett, Eur. Phys. J. B **14**, 747 (2000).
[19] T. Schroeder, J. B. Giorgi, A. Hammoudeh, M. B. N. Magg, and H.-J. Freund, Phys. Rev. B **65**, 115411 (2002); T. Schroeder, J. Aegenhagen, N. Magg, B. Immaraporn, and H.-J. Freund, Surf. Sci. **552**, 85 (2004).
[20] K. Radican, N. Berdunov, G. Manai, and I. V. Shvets, Phys. Rev. B **75**, 155434 (2007).
[21] A. Eichler and J. Hafner, Phys. Rev. Lett. **79**, 4481 (1997); A. Eichler, F. Mittendorfer, and J. Hafner, Phys. Rev. B **62**, 4744 (2000).
[22] A. Szabó, M. Kiskinova, and J. T. Yates, Jr., J. Chem. Phys. **90**, 4604 (1989).
[23] X.-Y. Zhu, S. R. Hatch, A. Campion, and J. M. White, J. Chem. Phys. **91**, 5011 (1989).

[24] I. N. Yakovkin, V. D. Osovskii, N. V. Petrova, and Yu. G. Ptushinskii, Surf. Rev. Lett. **13**, 375 (2006).
[25] K. H. Lau and W. Kohn, Surf. Sci. **75**, 69 (1978).
[26] T. L. Einstein, CRC Crit. Rev. Solid State Mater. Sci. **7**, 261 (1978).
[27] O. M. Braun and V. K. Medvedev, Sov. Phys. Usp. **32**, 328 (1989).
[28] N. V. Petrova and I. N. Yakovkin, Surf. Sci. **578**, 162 (2005).
[29] I. N. Yakovkin and N. V. Petrova, Surf. Sci. **600**, 2600 (2006).
[30] N. V. Petrova and I. N. Yakovkin, Eur. Phys. J. B **58**, 257 (2007).
[31] X. Gonze, J.-M. Beuken, R. Caracas, F. Detraux, M. Fuchs, G.-M. Rignanese, L. Sindic, M. Verstraete, G. Zerah, F. Jollet, M. Torrent, A. Roy, M. Mikami, Ph. Ghosez, J.-Y. Raty, and D. C. Allan, Comput. Mater. Sci. **25**, 478 (2002).
[32] N. Troullier and J. L. Martins, Phys. Rev. B **43**, 1993 (1991).
[33] J. P. Perdew, K. Burke, and M. Ernzerhof, Phys. Rev. Lett. **77**, 3865 (1996).
[34] A. Kiejna and R. M. Nieminen, J. Chem. Phys. **122**, 044712 (2005).
[35] L. M. de la Garza and L. J. Clarke, J. Phys. C **14**, 5391 (1981).
[36] H. J. Monkhorst and J. D. Pack, Phys. Rev. B **13**, 5188 (1976).
[37] N. V. Petrova, I. N. Yakovkin, and Yu. G. Ptushinskii, Low Temp. Phys. **31**, 300 (2005).
[38] N. V. Petrova, I. N. Yakovkin, and Yu. G. Ptushinskii, Surf. Sci. **497**, 349 (2002); Eur. Phys. J. B **38**, 525 (2004).
[39] N. V. Petrova and I. N. Yakovkin, Surf. Sci. **519**, 105 (2002).
[40] N. Metropolis, A. W. Rosenbluth, M. N. Rosenbluth, A. H. Teller, and E. Teller, J. Chem. Phys. **21**, 1087 (1953).
[41] J. Tersoff and D. R. Hamann, Phys. Rev. Lett. **50**, 1998 (1983); N. Lopez and S. Valeri, Phys. Rev. B **70**, 125428 (2004).
[42] T. L. Einstein, Surf. Sci. Lett. **84**, L497 (1979).
[43] I. N. Yakovkin, Surf. Sci. **577**, 229 (2005).
[44] B. Hammer, L. B. Hansen, and J. K. Norskov, Phys. Rev. B **59**, 7413 (1998).